

Structural study of the alkali-metal-induced (1×2) Ni(110) and $c(2 \times 4)$ Ni(110)/K/CO surface reconstructions

P. Statiris

Department of Physics and Astronomy and Laboratory for Surface Modification, Rutgers-The State University of New Jersey, Piscataway, New Jersey 08855-0849

P. T. Häberle

Departamento de Física, Universidad Técnica Federico Santa María, Casilla 110-V, Valparaíso, Chile

T. Gustafsson

Department of Physics and Astronomy and Laboratory for Surface Modification, Rutgers-The State University of New Jersey, Piscataway, New Jersey 08855-0849

(Received 24 September 1992)

The adsorption of alkali metals on fcc(110) surfaces is known to induce $(1 \times n)$ $n = 2, 3, \dots$ missing row (MR) reconstructions. We have used medium-energy ion scattering to study the structure of the (1×2) Ni(110)/K and the $c(2 \times 4)$ Ni(110)/K/CO surfaces. Our data for the (1×2) reconstruction are consistent with a MR structure. This reconstruction has the interesting feature that the first-to-second-layer separation (d_{12}) is *expanded* and not strongly contracted as has been observed for all other MR-reconstructed fcc(110) surfaces studied to date. For the $c(2 \times 4)$ Ni(110)/K/CO system, the structural parameters are very similar to those for the (1×2) system. Consequently, the $c(2 \times 4)$ symmetry is due to CO ordering on top of a MR reconstructed substrate.

I. INTRODUCTION

The (110) surface of fcc metals consists of close-packed rows of atoms running along the $[\bar{1}10]$ direction. The separation between rows along the [001] direction is larger by a factor of $\sqrt{2}$ than the distance between neighboring atoms within the rows. In this sense the (110) surface is the most "anisotropic" of all low-index fcc surfaces. The clean (110) surfaces of Au and Pt show reconstructions with (1×2) symmetry, which are different from the expected bulk termination (see Refs. 1 and 2 and references therein). In these reconstructions the surface unit cell is doubled along the (001) direction. Detailed studies have shown that both of them correspond to a structure in which every other close-packed row of atoms running along the $[\bar{1}10]$ direction is missing ["a missing row (MR) structure"]. Furthermore, small amounts of Cs have been shown to cause the Au(110) surface to reconstruct to a (1×3) MR reconstruction.³ Although the (110) surfaces of Ag, Cu, and Pd do not reconstruct when clean, adsorption of approximately 0.25 monolayers (ML) of alkali metals^{4,5} drives those surfaces to reconstruct to a (1×2) MR structure. Several different detailed structural studies of these surfaces have been made.^{6,7} It is by now also well established that the adsorption of sub-monolayer amounts of alkali metal on Ni(110) induces a doubling of the unit cell along the [001] direction. This structure has been claimed to be of the MR type,^{8,9} but no detailed structural study of this surface has been done to date.

Adsorption of CO on the K-covered Ni(110) (1×2) sur-

face at room temperature changes the surface symmetry from a (1×2) to a $c(2 \times 4)$ symmetry. Most studies^{10,11} performed on the $c(2 \times 4)$ structure have dealt with the arrangement of the CO molecules on the surface, while the substrate structure has not been studied in detail, despite its clear influence on the possible bonding sites available to the adsorbates.

In what follows we present the results of a structural study of the Ni substrate for both the (1×2) and $c(2 \times 4)$ reconstructions, and how the different adsorbates modify its structure. Our main experimental technique is medium-energy ion scattering (MEIS), which is well suited to determine the different structural models and parameters of this system.

Our study yields, besides detailed structural parameters for these surfaces, two unexpected results: The first-to-second-layer spacing (d_{12}) is expanded and the structural parameters for the two surfaces are very similar. A preliminary account of some of our results has appeared elsewhere.¹²

II. EXPERIMENT

A. The MEIS technique

In a MEIS experiment the probing ion beam, usually protons, is aligned along a major crystallographic direction (channeling) so that the ions can travel parallel to the atomic rows inside the crystal. For a perfect and rigid lattice only the first atom of each row would be hit by the incoming ions. Since the surface atoms do not allow

the ions to travel along the row direction, the incoming ions cannot scatter from deeper layer atoms. Atomic vibrations and distortions make it possible for the ions to penetrate the crystal along trajectories closer to the ion core rest positions. Even in this case the probability for an atom to be hit by an incoming ion decays very rapidly into the crystal. With 75-keV proton energy and channeling, this probability becomes negligible after the fourth atomic layer from the surface. The ions that backscatter off atoms below the first layer are subject to blocking from atoms closer to the surface. Therefore a reduction in the outgoing ion flux is observed along crystallographic directions. In a plot of yield versus scattering angle the reduction appears as a “blocking dip.” The shape and the size of the various dips are directly related to the structure of the surface. The scattering process itself is essentially a Rutherford-type collision off the screened potential of the atoms in the crystal. Since the scattering cross section is known for the energy range we are working in, one can calculate the number of atoms per surface unit cell that contribute to the scattering by simulating the whole scattering process using a computer. The simulations show that the backscattering yield depends chiefly on the positions and vibrational amplitudes of the surface atoms. One advantage of MEIS with respect to other structural techniques is that the simulation results can be compared directly to the experiment because both are obtained in absolute units. The agreement between the simulation results and the data for every set of parameters is checked with a χ^2 -type routine, until a set of parameters that gives the best fit in the different scattering geometries is found.

In our experiment ion scattering was done at room temperature using a proton beam. The proton energies used were 75 and 65 keV for the study of the Ni(110)/K and Ni(110)/K/CO surfaces, respectively. Working at these rather low energies provides a high surface sensitivity. The data presented were obtained with the beam-crystal-detector system in a channeling and blocking configuration. The channeling and blocking directions are usually chosen to be high symmetry directions within major crystallographic planes. Such planes are the $(1\bar{1}0)$, $(1\bar{1}1)$, and (001) and are referred to as the scattering zones.

B. Sample preparation

The sample was cleaned following standard UHV procedures. The cleanliness was monitored with Auger spectroscopy using a double-pass cylindrical mirror analyzer. At the end of the cleaning process the Auger signal of the most persistent contaminants (C and S) was less than 1% of a ML. Another way of checking the surface cleanliness of Ni(110) is by monitoring the surface relaxation. It has been observed in previous ion scattering work¹³ that contamination from the ambient, or from diffusion of bulk contaminants to the surface, is reflected directly in the surface relaxation. The clean surface shows a contraction of the first-interlayer spacing (d_{12}) by about 10%, which decreases with contamination. A typical ion scattering experiment in our setup could take up to 2 h. During

this time interval the *clean* surface contraction did not change, which we interpret to mean that the surface was free of contamination. Beam damage effects were negligible for the beam dose used (6×10^{15} protons/cm²).

The K source used for deposition was a commercially available SAES GETTERS source which was continuously outgassed throughout the duration of the experiment. At the time of deposition the pressure never exceeded 6×10^{-10} Torr. After deposition of $\sim 25\%$ ML of K and annealing to ~ 660 K a well-resolved low-background (1×2) low-energy electron diffraction (LEED) pattern was obtained. The K coverage measured with ion scattering was $25\% \pm 4\%$ ML per (1×1) unit cell. We have also tried varying the K coverage between 0.05 and 0.3 ML in an effort to reproduce previously reported LEED patterns⁵ and were successful in doing that. At 0.1 ML a well-resolved (1×3) pattern was observed, and from 0.15 to 0.30 ML the (1×2) pattern was present. To create a $c(2 \times 4)$ structure, the (1×2) surface was dosed with 6 L of CO (saturation coverage) and annealed to ~ 485 K.^{10,11} A few times during the course of the experiment we were able to see well-resolved $p(2 \times 2)$ LEED patterns which were uniform over the whole area of the sample. This happened just after the CO deposition and before annealing.

III. RESULTS

A. The scattering features of a MR reconstruction

From previous ion scattering work on the (1×2) MR reconstructions of (110) metal surfaces,^{1,2,7} it has become evident that there are two qualitative features in the ion scattering data that are characteristic of the MR structure. They are the increase in the depth of the [101] blocking dip in the $(1\bar{1}1)$ scattering zone and the decrease in the depth of the [116] dip in the $(1\bar{1}0)$ scattering zone.

Figure 1(b) is a side view of the $(1\bar{1}1)$ scattering plane, a plane that is very sensitive to the spacing between the first and second layer. Ions that backscatter off deeper layer atoms along the [101] direction will be blocked by atoms closer to the surface so a blocking dip is expected to occur at this scattering direction. Any change in the interlayer spacing should reflect in the angular position of this blocking dip. A reduction of the interlayer spacing (d_{12}) leads to a shift of the blocking dip to a lower scattering angle than the one expected in case of an ideal bulk termination (60°), while an increase of d_{12} produces the opposite effect.

The number of atoms directly visible to the incident ion beam in this scattering geometry is the same for the (1×1) and the MR (1×2) , because for every atom missing from the first layer another one is exposed in the second layer [Fig. 1(b)]. The backscattered yields away from the blocking direction should therefore be the same for the (1×1) and (1×2) MR structures. For the MR structure an ion backscattered from an exposed second-layer atom will be blocked by a first-layer atom. Thus, for this direction, the reduction in the yield is expected to be bigger in the case of a MR and this is a *fingerprint*

characteristic of a MR structure.

Another characteristic of the ion scattering from a MR is the reduction in the depth of the blocking dip along the $[11\bar{6}]$ direction in the $(1\bar{1}0)$ scattering zone [Fig. 1(c)].¹ Consecutive $(1\bar{1}0)$ planes terminate in the first and second layer as in Fig. 1(c). For the planes that terminate in the first layer, blocking occurs between first- and third-layer atoms. [Blocking also occurs between second- and fourth-layer atoms for the set of planes terminating in the second layer, but this does not change between the (1×1) and (1×2) MR structures. The blocking pattern observed in the experiments contains both contributions.] In the MR case, since every other atom along the (001) direction is missing [hatched atoms in Fig. 1(c)] there is no first-to-third-layer blocking along the $[11\bar{6}]$ direction [Fig. 1(c)]. This implies that the $[11\bar{6}]$ blocking dip for the (1×1) structure is expected to be deeper than for the (1×2) MR reconstruction.^{1,2}

In order to reduce the corrugation and smooth out the charge distribution induced by the missing row structure the surface layer usually relaxes towards the bulk. This

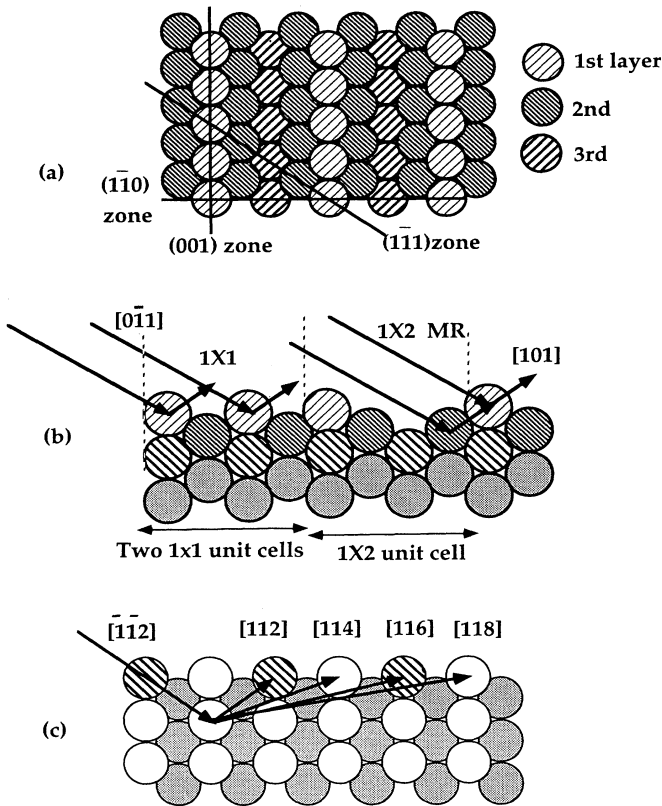


FIG. 1. (a) Top view of an fcc(110) MR surface. The different scattering zones are also shown. (b) Side view of the $(1\bar{1}1)$ scattering zone. The (1×1) and (1×2) MR unit cells are indicated. The incoming $([0\bar{1}1])$ and outgoing $([101])$ beam directions are indicated with arrows. (c) Side view of the $(1\bar{1}0)$ zone that includes the two inequivalent planes of atoms which contribute to the scattering (white and shaded atoms). In the case of a MR structure the hatched atoms are missing.

TABLE I. Systems that reconstruct to a MR and their surface relaxations. Δd_{ij} stands for change in the layer spacing between layers i and j .

System	Δd_{12}	Δd_{23}
Au (1×2) (Ref. 1)	-18%	+4%
Cs/Au (1×3) (Ref. 3)	-22%	-9%
Pt (1×2) (Ref. 2)	-16%	+4%
K/Ag (1×2) (Ref. 7)	-9%	-1%
Cs/Pd (1×2) (Ref. 6)	-9%	-1%
K/Ni (1×2)	+3%	-3%
Ni (1×1) (Ref. 13)	-9%	+3.5%
Ag (1×1) (Ref. 31)	-9.5%	+6%
Pd (1×1) (Ref. 32)	-6%	+1%

reduction of the interlayer spacing can be quite large; values from the literature for fcc(110) MR structures are contained in Table I.

B. The (1×2) Ni(110)/K surface

It has been claimed in previous LEED and photoemission studies^{8,9} that the structure of (1×2) Ni(110)/K is of the MR type, but no detailed structural analysis has been made to date. Studying this surface is also the first step necessary for understanding the coadsorption of CO on a surface already dosed with K.

Figure 2 contains ion scattering data collected around the $[101]$ direction in the $(1\bar{1}1)$ zone for the (1×1) and the (1×2) Ni(110) surfaces, together with a simulation for a MR structural model with parameters given below.

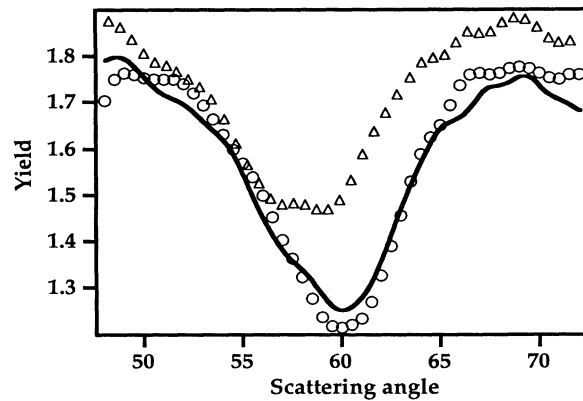


FIG. 2. Yield in atoms per (1×1) unit cell versus scattering angle (in degrees) in the $(1\bar{1}1)$ zone. The (1×1) data points are indicated with triangles, the (1×2) by circles, and the simulation based on the MR model with a solid line. The proton energy was 75 keV.

It can be seen that the scattering yield in the shoulders of the dips is almost the same for both structures, and that the (1×2) blocking dip is much deeper than the (1×1) one. Furthermore, the result of the simulation using a MR model with structural parameters as given below compares very well with the data (Fig. 2). Figures 3(a) and 3(b) show data from the $(1\bar{1}0)$ zone for the (1×1) and the (1×2) structures, respectively. The blocking dip in the $[116]$ direction is more pronounced in the case of the (1×1) surface. As discussed above, this feature also is related to a MR-type structure.

A contraction of d_{12} would shift all blocking dips to scattering angles smaller than the ones expected in the case of an ideal bulk termination. The shift is clear in the data for the clean nickel surface (Fig. 2). These data are consistent with a 10% contraction of the first-layer separation, in good agreement with previous results.¹³ A shift to lower scattering angles has also been observed in all MR reconstructions studied so far (Table I). However, for the K/Ni(110) (1×2) structure, no shift to lower scattering angles is observed; thus no contraction takes place. In fact, after fitting the data we found a *slight expansion* of d_{12} (Table II). A complete set of structural parameters is given in Table II. Figure 4 shows a side view of the MR structure in the $(1\bar{1}1)$ zone where all the relaxations are included. Only a few other systems have been reported to show an expansion of d_{12} and none of them is a MR structure.^{14,15} In the case of Pd(100), where an expansion of d_{12} is found with LEED,¹⁴ the presence of interstitial hydrogen and the presence of magnetic moments

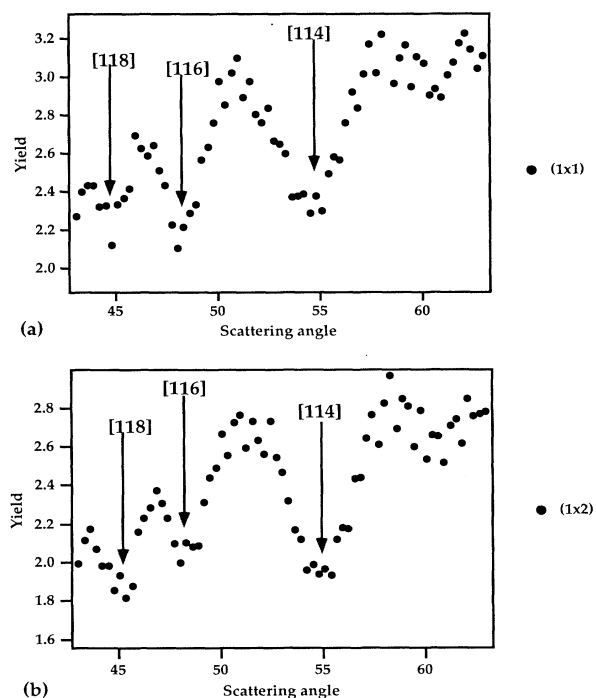


FIG. 3. (a) and (b) Plot of the yield in atoms per (1×1) unit cell versus angle (in degrees) in the $(1\bar{1}0)$ zone for the (1×1) and (1×2) surfaces, respectively. The proton energy was 75 keV.

TABLE II. The detailed relaxation parameters for the (1×2) and $c(2 \times 4)$ structures. Changes in layer spacing are indicated as in Table I, while B_3 stands for buckling in the third layer. The error bar is 1% for Δd_{12} and Δd_{23} , and 2% for Δd_{34} and B_3 .

	(1×2)	$c(2 \times 4)$
Δd_{12}	+3%	+4%
Δd_{23}	-3%	-2%
Δd_{34}	+2%	+2%
B_3	+2%	+3%

on the surface are considered as possible reasons for this unusual relaxation. For the case of beryllium an expansion of 5.8% of the first-interlayer spacing was found.¹⁵ First-principles calculations on a Be dilayer yield a 5% increase of the interplanar spacing.¹⁶ A more recent calculation for a thick slab yields 3.9% and 2.2% expansion, respectively, for the first-to-second- and second-to-third-layer separations.¹⁷ The unusual (in sign and magnitude) relaxation of the Be(0001) surface is due to the unique bonding characteristics of Be. A more detailed discussion can be found in Refs. 15–17.

The fact that the yields at the shoulders (Fig. 2) are the same means that the K atoms cannot be sitting in lattice sites as they would then shadow the Ni atoms underneath, reducing the yield on the shoulders. From our experimental data we have not been able to unambiguously locate the binding site of the K atoms. Since no blocking is observed for the K spectra, the K atoms are most probably located along the troughs created by the MR (Ref. 5) far from any high symmetry positions.

In a further effort to locate the alkali-metal atoms on the surface we also studied adsorption of Cs on the Ni(110) surface. Cs has a much higher scattering cross section than K, thus the effect it should have on the scattering spectra is much more pronounced. A well-resolved (1×2) LEED pattern results after deposition of 0.25 ML of Cs. The MR structure fits the Cs/Ni(110) data very well and d_{12} is *expanded* for this system also. Despite the large Cs cross section, we could not observe any blocking features in the Ni spectra that could be assigned to Cs. Moreover, the Cs spectra themselves do not show any blocking features. In fact, comparing data for the K- and Cs-induced (1×2) reconstructions we could not see any significant difference either in the yields or in the positions and shapes of the blocking dips. We interpret

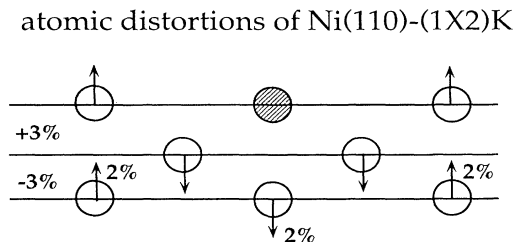


FIG. 4. Side view in the $(1\bar{1}1)$ zone of the MR surface. The arrows indicate the motion of the atomic planes.

this to mean that Cs (and K) atoms stay on top of the surface, far from high symmetry positions.

C. The $c(2 \times 4)$ Ni(100)/K/CO surface

Angle-resolved x-ray photoemission-spectroscopy shows that CO adsorbs on a K-dosed Ni(110) surface with its molecular axis tilted about 30° off the surface normal along the [001] direction.¹¹ Furthermore, a thermal desorption spectroscopy (TDS) study shows that a new CO desorption peak appears on the K-covered surface which can be directly associated with CO molecules affected by the presence of K.¹⁰ This desorption peak occurs at a higher temperature than the one due to CO desorption from the clean Ni(110) surface, indicating a stronger CO bonding to the surface when K is present. Moreover the area under this peak is found to correspond to almost twice the amount of K adsorbed.

Figures 5(a) and 5(b) contain both our (1×2) and $c(2 \times 4)$ data. The scattering geometry for the data in Fig. 5(a) is the same as that in Fig. 2. Figure 5(b) shows the data collected around the [112] direction in the $(1\bar{1}0)$ zone [Fig. 1(c)]. The positions and depths of the blocking dips are very similar in both graphs. The yields in the case of the $c(2 \times 4)$ structure are a little higher than for the (1×2) in the $(1\bar{1}1)$ zone. In this zone the contribution to the scattering yield comes mainly from the first and second layers. The small difference in the yield could be explained by an enhancement of the vibrational amplitude of the first-layer atoms which increases the visibility of the second layer and consequently increases the

yield. For the CO-covered $c(2 \times 4)$ surface a slight shift to higher scattering angles of the (101) blocking dip can be seen in Fig. 5(a). This corresponds to a further expansion of d_{12} ($1\% \pm 1\%$) upon CO adsorption, as can be seen from Table II. The similarity of the data in the $(1\bar{1}1)$ and $(1\bar{1}0)$ zone is a first indication that the substrate has a structure very similar to the (1×2) surface.

We have done simulations to determine the position of the CO molecules on top of the surface by including the effect of scattering from the CO molecules. Since the cross sections for C and O are low with respect to Ni, the effect of the CO in the scattering spectra is not expected to be pronounced. As the CO molecules lie along the [001] direction,¹¹ the $(1\bar{1}0)$ scattering zone data are the most sensitive to the presence of CO, and our simulations confirm this trend. The CO coverage was taken to be twice that of K,¹⁰ and a MR structure was assumed for the substrate. The parameters varied in the simulations were the tilt of the CO molecules with respect to the surface normal and the bonding site. The bond lengths were taken from Ref. 18. Assuming a range between 20° and 40° for the tilt of the axis of the CO molecules with respect to the surface normal, we found better agreement with the data when the CO molecules were bonded onto the second layer rather than the first. The simulations for the $c(2 \times 4)$ surface are consistent with CO molecules located within the troughs of the missing rows in the $(1\bar{1}0)$ planes with a tilt angle of $30^\circ \pm 5^\circ$, in good agreement with previous results.¹⁹ The CO molecules are in effect sitting almost perpendicular to the microfacets created

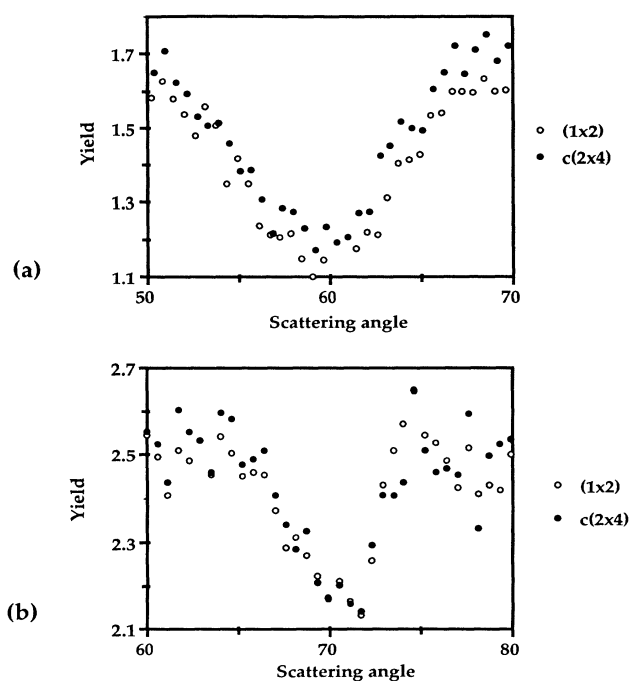


FIG. 5. (a) and (b) Comparison of the (1×2) data (circles) with the $c(2 \times 4)$ data (filled circles) for the $(1\bar{1}1)$ and $(1\bar{1}0)$ scattering zones, respectively. Yield is in atoms per unit cell and scattering angle is in degrees. The proton energy was 65 keV.

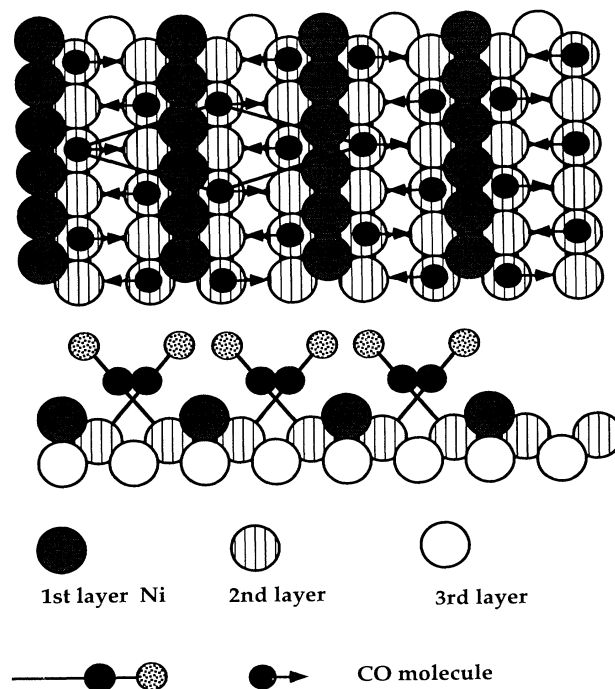


FIG. 6. Top and side view of a possible arrangement of the CO molecules on top of the MR reconstructed substrate. The direction of the arrows indicates the tilt direction of the CO molecules. The tilt angle is $30^\circ \pm 5^\circ$.

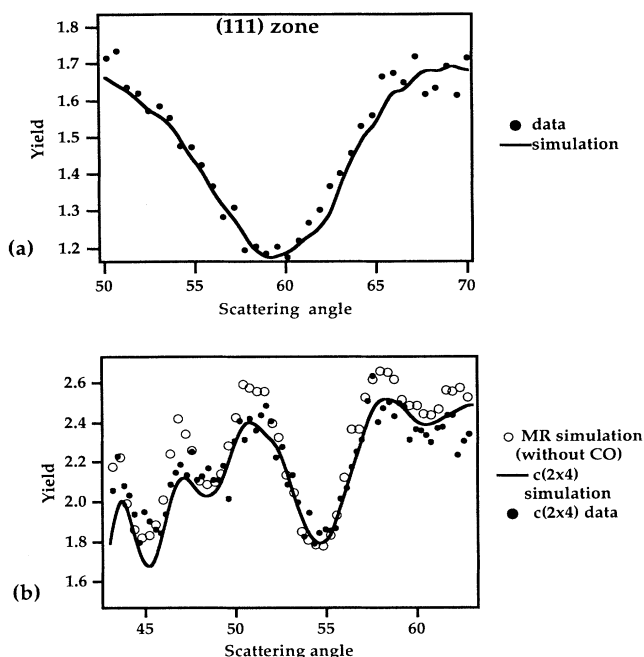


FIG. 7. (a) and (b) Comparison between data (dark circles) and simulation (solid line) for the $c(2 \times 4)$ structure, in the $(1\bar{1}1)$ and $(1\bar{1}0)$ zones, respectively. Yield is in atoms per unit cell and scattering angle is in degrees. The proton energy was 65 keV.

by the MR, and they are contained in the $(1\bar{1}0)$ planes (Fig. 6). The agreement with the data improves slightly if we rigidly shift the CO molecules along the microfacet towards the third layer atoms by 10% of the interplanar spacing. Figure 7 shows the $c(2 \times 4)$ data and simulations based on the MR structure. Figure 7(b) contains two simulations: The solid line is the simulation result assuming CO presence in the surface (CO coverage 0.5 ML) and the open circles represent the simulated yield for the best-fit MR model. The simple MR simulation evidently overestimates the shoulders between the blocking dips. The structural parameters agree within 2% with the ones for the (1×2) structure. Within that limit we cannot observe any lateral movements of the atomic rows.

The MR model for the Ni substrate can explain why the CO atoms seem to sit in a tilted position on the surface. It is well established that CO adsorbs in a perpendicular configuration on Ni(100) and (111). One can assume then that the CO atoms are sitting on the (111) facets created by the MR in an almost vertical position, in which case the tilt would be (relaxations not taken into account) 35.3° off the surface normal corresponding to the angle between the $[110]$ and $[111]$ directions.

D. Vibrational anisotropy

The number of atoms visible to the ion beam depends, among other things, on the vibrational ampli-

tude of the surface atoms. Since for the atoms residing on the surface, half of the nearest-neighbor bonds are broken, the vibrational amplitudes are expected to be enhanced with respect to the bulk. Previous studies have shown that this is indeed the case and, moreover, anisotropic vibrational amplitudes have been found in different experiments.^{20,21}

A three-dimensional ellipsoid can be used to represent the vibrational amplitudes in all directions. Since an ion traveling parallel to a row of atoms is sensitive to the displacement of the atoms in the direction perpendicular to the row, the relevant vibrational amplitudes for a particular ion beam direction are given by the intersection of the ellipsoid with the plane normal to this direction. To probe the vibrational amplitude of atoms within the surface plane one has to be channeling along the surface normal. Our normal-incidence data are shown in Fig. 8. We have found that using isotropic vibrations we cannot satisfactorily fit the normal-incidence data. The difference between the normal-incidence data and all other data sets is that for the latter the path of the incoming ions is very similar to the path of the outgoing ones. This in turn means that the effect of vibrations is the same for ions that travel in or out the crystal. For the normal-incidence data the ions see two different cross sections of the vibrational ellipsoid depending on their direction with respect to the surface normal. We have done simulations using anisotropic vibrations and we found that the vibrational amplitude perpendicular to the surface is 35–40% larger than in the plane (the in plane vibrations are enhanced by about 50% over the bulk value). Figure 8 contains the normal-incidence data and the simulation result using anisotropic vibrations.

The displacements of atoms within a row are correlated. The net effect of correlation is to reduce the effective vibrational amplitude of the atoms.²² Taking correlated vibrations into account, the in plane vibrations are enhanced by a factor of 3 and the out of plane ones were enhanced by a factor of 4. Previous MEIS studies

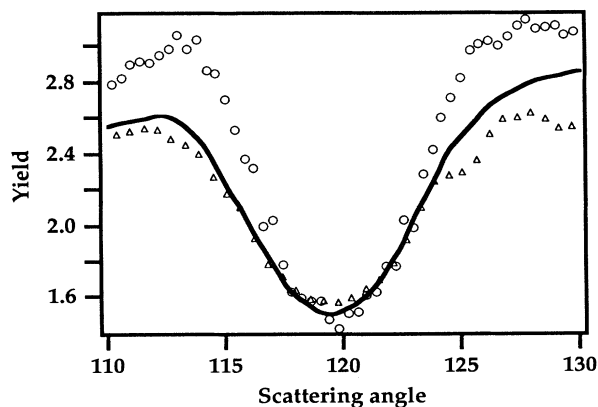


FIG. 8. Comparison between data and two different simulations for the normal incidence data in the $(1\bar{1}1)$ zone. The data points are represented by triangles. The solid line corresponds to a simulation using anisotropic vibrations while the circles correspond to a simulation that uses isotropic vibrations.

on (1×1) Ni(110) at room temperature^{13,23} have found the surface vibrational amplitudes to be less than twice the bulk value. In a recent LEED study of the thermal roughening of the Ni(110) surface²⁴ it was found that between 470 and 900 K the out of plane vibrations were enhanced by a factor of 3 while the in plane ones by a factor of 15, which is much larger than our, as well as previous, MEIS results.²³

IV. DISCUSSION

According to first-principles calculations²⁵ on Au(110), it is energetically favorable for this surface to reconstruct to a MR (1×2) structure. Similarly the addition of electronic charge onto the Ag(110) surface induces a MR reconstruction.²⁶ In the traditional picture of bonding of alkali-metal atoms to metal surfaces, the alkali metals act as charge donors to the surface. The lowering of the work function is usually seen as supporting this idea.²⁷ The theoretical calculation done on Ag(110) suggests that charge donation may be the reason why some (110) metal surfaces reconstruct to a (1×2) MR structure upon alkali-metal adsorption. The fact that the surface area increases when a MR reconstruction occurs is important for lowering the surface energy. In very rough terms the free surface electrons have more space to move when the surface area increases and this lowers their kinetic energy.^{25,26}

No easy explanation can be given to why Ni(110) does not follow the oscillatory relaxation pattern starting with a contraction of d_{12} observed for Cu, Pd, Pt, Ag, and Au. The alkali-metal atoms most probably reside along the troughs created by the missing rows. The ionic radius of K is 1.33 Å while the atomic one is 2.26 Å, and previous studies have shown^{28,29} that a value of about 2.0 Å is a reasonable value for the K radius. Since the alkali-metal ions have a much larger size than Ni atoms, they should be located above the first-layer Ni atoms. What we observe in the experiment is an increase in d_{12} , which implies that the atoms are being pushed apart away from their original positions. From the point of view of electrostatics this can be achieved if the repulsive forces between the Ni ion cores are somehow increased. A possible model is the following: Upon K adsorption there is charge redistribution and the electron density is locally increased between the Ni and K atoms while the electronic charge density in the first and second nickel layers is decreased. Since in this situation electron screening is not as effective the repulsive forces between nuclei push the Ni atoms apart resulting in an increase of d_{12} and decrease of d_{23} .

What holds true for most surfaces is that the first layer seems to "want" to relax towards the bulk (d_{12} is decreased). The driving force for this reconstruction is of electrostatic nature.³⁰ The electron density at the surface is rearranged in a way that the corrugation induced by the presence of the surface is smoothed out and this in turn leads to the observed relaxations of the atoms (Smoluchowski smoothing). Looking at the values of the relaxation parameters in Table I it is evident that, although for the case of clean surfaces (reconstructed or not^{31,32}) the sign of the relaxations is what theory pre-

dicts, namely a contraction of d_{12} followed by expansion of d_{23} , for all the alkali-metal-dosed surfaces contraction is followed by another contraction. Since for the alkali-metal-dosed surfaces both effects are present, the measured relaxations reflect the superposition of the two effects. We believe that the sign change in d_{23} is due to the presence of alkali metal. It is easier to see this effect in the sign change of d_{23} since it is usually a smaller number than d_{12} . The sign change is also evident by comparing Au (1×2) and K/Au (1×3) . The fact that for the Ni(110) surface d_{12} is expanded could be due to the fact that the charge redistribution is so drastic that it overcomes the Smoluchowski smoothing. Alternatively, one could look for an explanation for the anomalous expansion of d_{12} along the lines of Quinn *et al.*¹⁴ One explanation for the expansion of d_{12} on Pd(100) proposed by them was the presence of magnetic moments in the surface, an idea that goes back to the concept of a magnetic pressure. This notion would in our case imply the existence of enhanced magnetic moments at the alkali-metal-induced (1×2) surface, a speculation that should be possible to test using spin-sensitive surface spectroscopies. The similarity of our results for K and Cs adatoms [and the different behavior for Ni (1×2) and Ag (1×2) (Ref. 7)] does suggest that the origin for the anomalous expansion is related to the electronic structure of the Ni atoms.

We have shown that for both (1×2) and $c(2 \times 4)$ Ni(110) the structure of the substrate is very similar. The structural changes induced on the system seem to be chiefly due to alkali-metal adsorption. These local changes in structure upon the adsorption of very small amounts of alkali-metal are demonstrated in a recent STM study of K on Cu(110).³³

The question of how the $c(2 \times 4)$ structure comes about upon adsorption of CO can be answered in simple terms with our data. According to previous work,¹⁰ the CO coverage is almost twice that of K. The K coverage on the surface measured with MEIS is 0.25 ML, implying a CO coverage around 0.5 ML. The CO molecules could either bond to the first-layer Ni atoms or to the exposed (because of the MR) second-layer atoms. A $c(2 \times 4)$ structure like the one shown in Fig. 6 is clearly favored by a MR structure where the second-layer atoms of the substrate contribute possible bonding sites. Since there is not enough space to accommodate two CO molecules bonded to two second-layer nickel atoms, which are directly opposite each other across the missing rows, the CO molecules are arranged in a zigzag-type chain along each missing row. The $c(2 \times 4)$ symmetry of the surface comes about with the arrangement of Fig. 6. The attractive feature about this configuration is that all the possible sites for CO adsorption are occupied and two coexisting $c(2 \times 4)$ domains are created giving a coverage of 0.5 ML for CO.

V. CONCLUSIONS

We have studied the structure of the (1×2) Ni(110)/K and the $c(2 \times 4)$ Ni(110)/K/CO systems. Our data show

that in both cases the Ni substrate arranges itself to a MR structure and a small *expansion* of d_{12} is found. Since we have observed no lateral movement (within the limits of our measurements) of the Ni substrate atoms upon coadsorption of CO, we believe that the $c(2 \times 4)$ pattern observed in the case of coadsorption is due to an ordering of the CO molecules on top of a (1×2) reconstructed substrate.

ACKNOWLEDGMENTS

We would like to thank Professor T. Madey for providing us with the Ni crystal and Dr. Q.T. Jiang for many helpful hints and discussions. This research was jointly supported by NSF Grants Nos. DMR-9019868, and INT-9121013, FONDECYT Grant No. 0480-90, and UTFSM Grant No. 921101 Chile.

- ¹M. Copel and T. Gustafsson, Phys. Rev. Lett. **57**, 723 (1986).
- ²P. Fenter and T. Gustafsson, Phys. Rev. B **38**, 10197 (1988).
- ³P. Häberle, P. Fenter, and T. Gustafsson, Phys. Rev. B **39**, 5810 (1989).
- ⁴B.E. Hayden, K.C. Prince, P.J. Davie, G. Paolucci, and A.M. Bradshaw, Solid State Commun. **48**, 325 (1983).
- ⁵R.L. Gerlach and T.N. Rhodin, Surf. Sci. **17**, 32 (1969).
- ⁶C.J. Barnes, M. Lindroos, and D.A. King, Surf. Sci. **201**, 108 (1988).
- ⁷J.W.M. Frenken, R.L. Krams, and J.F. van der Veen, Phys. Rev. Lett. **59**, 2307 (1987).
- ⁸N. Memmel, G. Rangelov, E. Bertel, and V. Dose, Phys. Rev. B **43**, 6938 (1991).
- ⁹K. Flynn, K.D. Jamison, P.A. Thiel, G. Ertl, and R.J. Behm, J. Vac. Sci. Technol. A **5**, 794 (1987).
- ¹⁰L.J. Whitman and W. Ho, J. Chem. Phys. **83**, 4808 (1985).
- ¹¹D.A. Wesner, F.P. Coenen, and H.P. Bonzel, Phys. Rev. Lett. **60**, 1045 (1988).
- ¹²Q.T. Jiang, P. Statiris, P. Häberle, D.M. Zehner, and T. Gustafsson, J. Vac. Sci. Technol. A **10**, 2197 (1992).
- ¹³S.M. Yalisove, W.R. Graham, E.D. Adams, M. Copel, and T. Gustafsson, Surf. Sci. **171**, 400 (1986).
- ¹⁴J. Quinn, Y.S. Li, D. Tian, H. Li, and F. Jona, Phys. Rev. B **42**, 11348 (1990).
- ¹⁵H.L. Davis, J.B. Hannon, K.B. Ray, and E.W. Plummer, Phys. Rev. Lett. **68**, 2632 (1992).
- ¹⁶J.C. Boettger and S.B. Trickey, Phys. Rev. B **32**, 1356 (1985).
- ¹⁷P. Feibelman, Phys. Rev. B **46**, 2532 (1992).
- ¹⁸D.J. Hannaman and M.A. Passler, Surf. Sci. **203**, 449 (1988).
- ¹⁹*Physics and Chemistry of Alkali Metal Adsorption*, edited by D.A. Wesner, F.P. Coenen, and H.P. Bonzel (Elsevier Science, London, 1989).
- ²⁰Q.T. Jiang, P. Fenter, and T. Gustafsson, Phys. Rev. B **44**, 5773 (1991).
- ²¹J.W.M. Frenken, J.F. van der Veen, and G. Allan, Phys. Rev. Lett. **51**, 1876 (1983).
- ²²R.S. Nelson, M.W. Thompson, and H. Montgomery, Philos. Mag. **7**, 1385 (1962).
- ²³J.F. van der Veen, G.R. Smeenk, M.R. Tromp, and F.W. Sarris, Surf. Sci. **79**, 212 (1979).
- ²⁴Y. Cao and E.H. Conrad, Phys. Rev. Lett. **64**, 447 (1990).
- ²⁵K.M. Ho and K.P. Bohnen, Phys. Rev. Lett. **59**, 1833 (1987).
- ²⁶C.L. Fu and K.M. Ho, Phys. Rev. Lett. **63**, 1617 (1989).
- ²⁷A. Zangwill, *Physics at Surfaces* (Cambridge University Press, Cambridge, 1988).
- ²⁸P. Häberle and T. Gustafsson, Phys. Rev. B **40**, 8128 (1989).
- ²⁹U. Muschiol, P. Bayer, K. Heinz, W. Oed, and J.B. Pendry, Surf. Sci. **275**, 185 (1992).
- ³⁰R. Smoluchowski, Phys. Rev. **60**, 661 (1941).
- ³¹E. Holub-Krappe, K. Horn, J.W.M. Frenken, R.L. Krams, and J.F. Van der Veen, Surf. Sci. **188**, 335 (1987).
- ³²C.J. Barnes, M.Q. Ding, M. Lindroos, and D.A. King, Surf. Sci. **162**, 59 (1985).
- ³³R. Schuster, J.V. Barth, G. Ertl, and R.J. Behm, Surf. Sci. **247**, L229 (1991).